

This is the accepted version of the following article:

Roche, E. T., Wohlfarth, R., Overvelde, J. T. B., Vasilyev, N. V., Pigula, F. A., Mooney, D. J., Bertoldi, K. and Walsh, C. J. (2014), A Bioinspired Soft Actuated Material. *Adv. Mater.*, 26: 1200–1206.

which has been published in final form at <http://dx.doi.org/10.1002/adma.201304018>.

Copyright WILEY-VCH Verlag GmbH & Co. KGaA, 69469 Weinheim, Germany, 2013

# **ADVANCED MATERIALS**

## Supporting Information

*For Adv. Mater., DOI:10.1002/adma.201304018*

### A Bioinspired Soft Actuated Material

*Ellen T. Roche, Robert Wohlfarth, Johannes T.B. Overvelde, Nikolay V. Vasilyev, Frank A. Pigula, David J. Mooney, Katia Bertoldi, and Conor J. Walsh\**

Supporting Information for

## A Bioinspired Soft Actuated Material

Authors: Ellen T. Roche<sup>1,2</sup>, Robert Wohlfarth<sup>3</sup>, Johannes T.B. Overvelde<sup>1,4</sup>, Nikolay V. Vasilyev<sup>5</sup>, Frank A. Pigula<sup>5</sup>, David J. Mooney<sup>1,2</sup>, Katia Bertoldi<sup>1,4</sup>, and Conor J. Walsh<sup>1,2\*</sup> (\*corresponding author)

[\*] Professor Conor J. Walsh, Ellen T. Roche, Professor David J. Mooney  
<sup>1</sup>School of Engineering and Applied Sciences, Harvard University, Pierce Hall, 29 Oxford Street, Cambridge, MA 02138 (USA)  
<sup>2</sup>Wyss Institute for Biologically Inspired Engineering, Harvard University, 3 Blackfan circle, Boston, MA 02155 (USA)  
E-mail: [walsh@seas.harvard.edu](mailto:walsh@seas.harvard.edu)

Robert Wohlfarth  
<sup>3</sup>Technical University of Munich, Germany, Arcisstr. 19, D-80333 Munich (Germany)

Johannes T.B. Overvelde, Professor Katia Bertoldi  
<sup>1</sup>School of Engineering and Applied Sciences, Harvard University, Pierce Hall, 29 Oxford Street, Cambridge, MA 02138 (USA)  
<sup>4</sup>Kavli Institute for Bionano Science and Technology, Harvard University, 29 Oxford Street, Cambridge, MA 02138 (USA)

Dr. Nikolay V. Vasilyev, Dr. Frank A. Pigula  
<sup>5</sup>Department of Cardiac Surgery, Children's Hospital Boston, 300 Longwood Ave, Boston, Massachusetts 02115 (USA)

Keywords: Soft actuated material, embedded actuators, pneumatic actuators, biomimetic motion, Three-dimensional motion

## **Table of Figures in Supporting Information**

Figure S1: Actuator/PAM Fabrication

Figure S2: Actuator/PAM Characterization

Figure S3: Test Specimen Fabrication

Figure S4: Test Specimen Characterization

Figure S5: Additional Test Specimen Characterization

Figure S6: Left Ventricle Physical Prototype Fabrication

Figure S7: Left Ventricle Mold Dimensions

Figure S8: Test Set-Up with EM trackers for measuring motion

## **Table of Movies in Supporting Information**

Movie S1: Actuator Behaviour on Pressurization

Movie S2: Test Specimen Strain Tracking and FE Simulation

Movie S3: FE Model of Left Ventricle Prototype

Movie S4: Physiological Motion of Left Ventricle Prototype

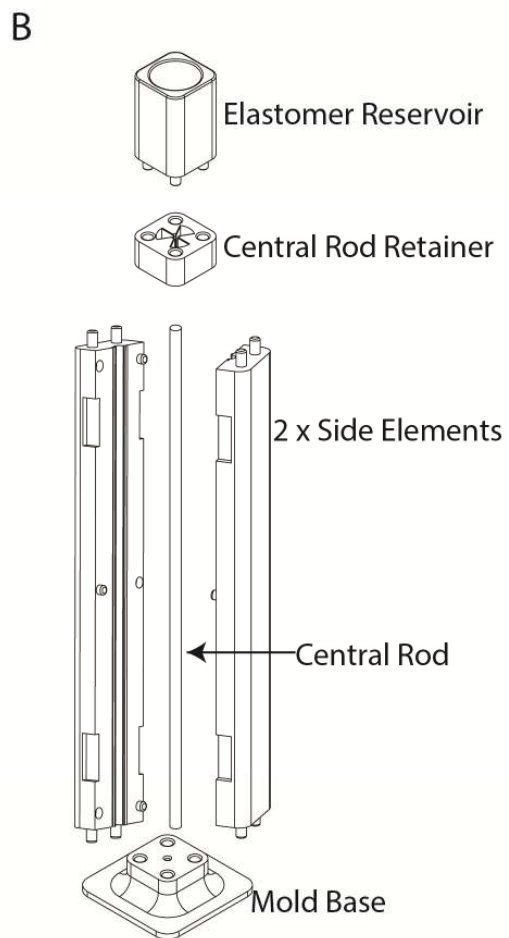
Movie S5: Active Left Ventricle Prototype and Numerical Model

Movie S6: Pathological Motion of Left Ventricle Prototype

Movie S7: FE Model of Pathological Motion

## 1 Actuator Fabrication

The plastic molds for the elastomeric components were designed as shown in Figure S1. The molds were 3D printed on an Object Connex 500 printer using Vero material (Fig. S1A). A 4mm hole was manually drilled into the cylindrical cavity through the wall of one of the side components of the mold for injection of prepolymer. The mold was assembled (Fig. S1B, C) and teflon tape was used to seal seams between mold components. Ecoflex 00-30 (Smooth-on Inc.) was mixed and degassed in an ARE-250 mixer (Thinky), then molded into a tube of the following dimensions; inner diameter 1.6mm and outer diameter 3.5mm as detailed in the following paragraph. Uncured elastomer was poured into the open end of a 3cc syringe, ensuring not to introduce air. The syringe was connected to a female luer lock extension line (Qosina 26219) shortened to 5cm. The line was primed to remove air and inserted into the drilled hole (Fig S1C). Once the cavity had been completely filled, the central rod (1.6mm diameter stainless steel rod) was then slowly inserted through the upper central rod retainer, and into the base. The mold was cured in a pressure chamber at 100psi for two hours. The elastomeric tube was demolded and advanced to the end of central rod. One end of the tube was closed with Ecoflex 00-30 and cured quickly with a heat gun. The tube was then completely removed from the central rod and cut to 75mm length (Fig S1-D) A section of mesh (Techflex PTN 0.13) was cut to a length of 75mm and its ends were heated with a flame and brass forming tool to prevent fraying at one end and to close the mesh at the other end. The mesh was placed over the molded tube. The open end was advanced over a length of air supply tube (McMaster Carr Silicone tubing 1/8 inch tubing 5236K502) until the air supply tube extended 10mm inside the molded tube. Nylon thread or suture material was used to secure mesh and molded tube onto the air supply tube. The assembly was roll-coated with a thin layer of Ecoflex excess material was removed with a spatula. Finally, the assembled actuator was cured with a heat gun and left for two hours for full curing of the polymer.



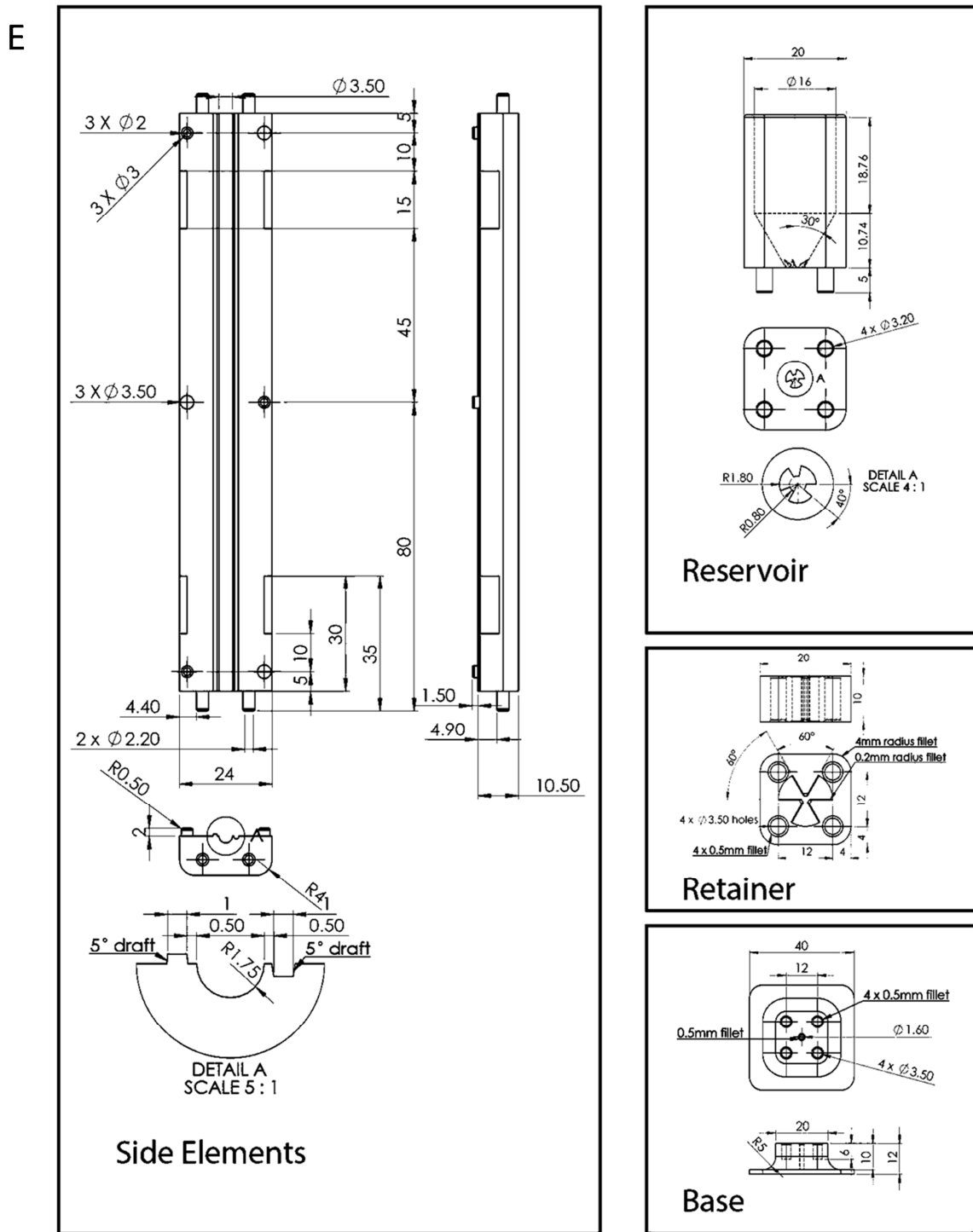


**Figure S1:** A) 3-D printed mold components (printed on Objet Connex 500 in Vero clear, vero black and vero white materials) B) Mold components C) Injection of uncured elastomer D) 75mm lengths of molded tube and mesh E) Dimensions of mold components

## 2 Actuator Characterization

In addition to characterizing longitudinal contraction and radial expansion of the actuators, we measured stiffness experimentally and measured the effect of increasing pressure on actuator axial stiffness. The test sequence is shown in Figure S1A. An Instron 5566 tensile testing machine was used for force measurements. An actuator was clamped by each end in the tensile tester at a grip-to-grip spacing of 50mm without blocking the air supply tube. The actuator was pressurized to a set value and the crosshead lowered until the force reading was zero (Fig S2A Step1-2). The crosshead was moved up to the original gauge length while measuring force (Fig S2A Step2-3). The force/displacement curve for the latter step was plotted for pressure increments of 0,5,10, 15 and 20psi (Fig S2B). The slope of the force/displacement curve was calculated for each pressure (Fig S2B). As the values were similar for each pressure the value of force/displacement at 10psi was used to calculate Young's modulus (E) for input into the finite element model (Fig S2D). The slope was 0.70N/mm, giving a value for E of 1.78MPa as detailed in Equation 1 below where  $d_0$  is original gauge length (50mm),  $A_0$ =circular cross area for a radius of 2.5mm (final nominal diameter of actuator is 5mm), F= force,  $\sigma$ = stress ( $\text{N}/\text{mm}^2$ ) and  $\varepsilon$ = strain

$$E = \frac{\sigma}{\varepsilon} = \frac{F/A_0}{\Delta d/d_0} = \frac{F}{\Delta d} * \frac{d_0}{A_0} = 0.70 * \frac{50}{\pi(2.5)^2} = 1.78 \frac{N}{\text{mm}^2} = 1.78 \text{MPa} \quad [1]$$

This value was used as input for the FE model for the material properties of the actuators.

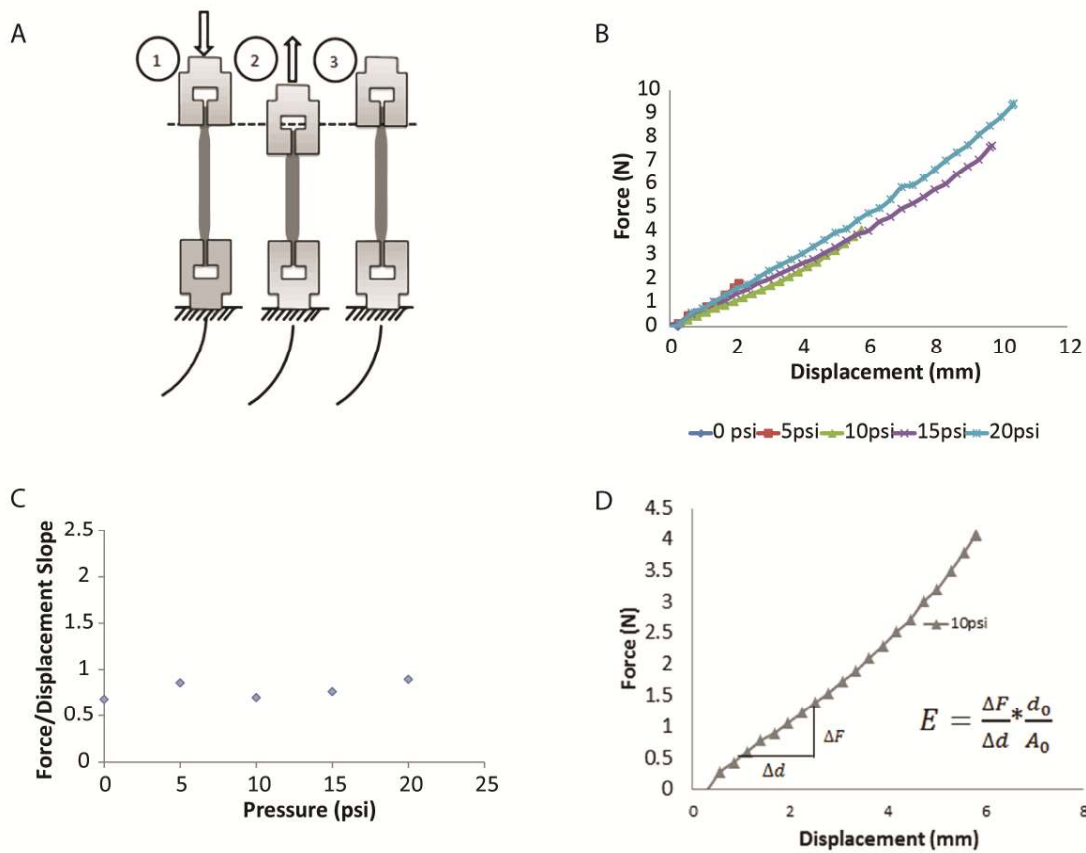


**Figure S2:** A) Test set-up for measuring stiffness of actuators. Actuator is pressurized (1) then crosshead is lowered until force reading is zero (2). Crosshead is returned to starting point (3) while measuring force. B) Force displacement slopes for actuators at 0, 5,10,15 and 20psi. C) Slope of force/displacement curve for different pressures showing similar slopes for each pressure. D) Calculation of Young’s Modulus (E) from the force /displacement curve for 10psi.

### 3 Test Specimen Fabrication

Multiple test specimens were fabricated as described in Figure S3 using a two-part mold. For multiple (3) actuator specimens,  $W=S*2+20\text{mm}$  (where  $S$  = spacing and 20mm is the sum of 2.5mm between outer actuators and edge and  $5\text{mm}*3$  for each actuator). Spacing ( $S$ ) is expressed in terms of nominal diameter of actuator ( $D$ ).

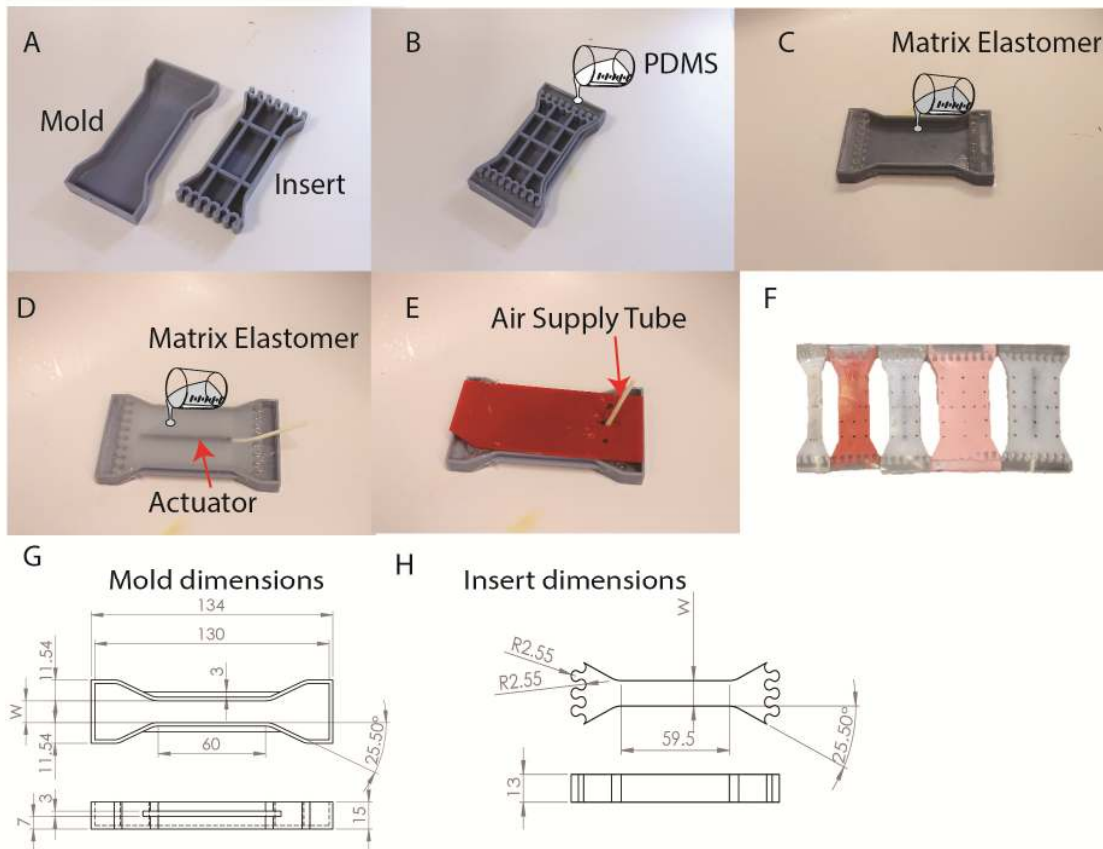


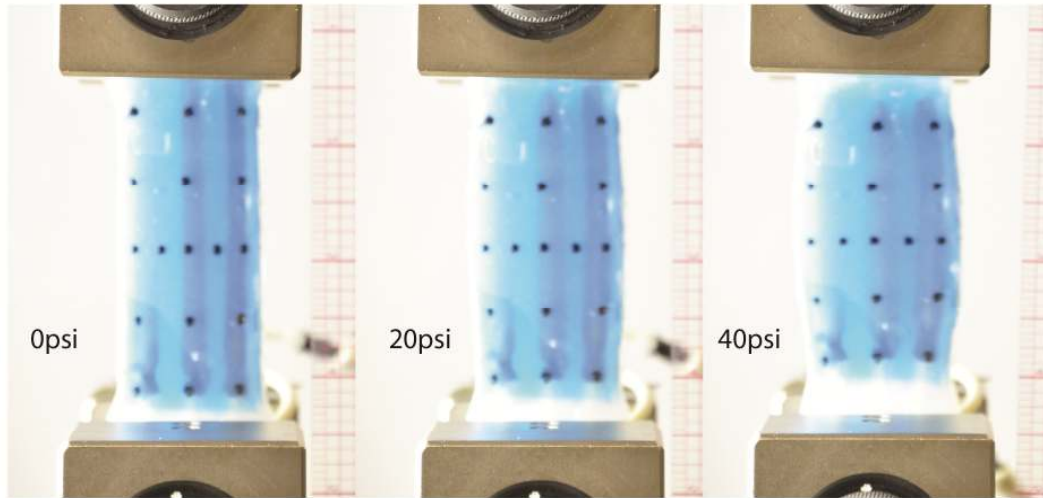
**Figure S3:** A) We 3-D printed parts of mold (printed in Vero blue on Objet Connex 500) B) We poured Polydimethylsiloxane (PDMS, Sylgard 184, Dow Corning) into ends of molds C) We removed insert to leave PDMS ends in molds, and poured a 4mm layer of Ecoflex 00-30 (Smooth on Inc.) or Elastosil M4601 (Wacker Chemie AG). D) We aligned actuator in centre (or multiple actuators at desired spacing). We used small amounts of uncured polymer

and a heat gun were used to fix actuators in place until final pour of Ecoflex 00-30 or Elastosil M4601 to top of mold E). We then covered the mold while curing to prevent air supply tube from being embedded in the test specimen matrix. F) The process was repeated for different matrix widths, actuator spacings and materials. Optical trackers were marked on specimens with permanent marker using laser cut stencil. Markers were placed as follows; 5 rows, 3 or 5 columns (midline and 5mm bilateral offsets from midline). Vertical spacing was 5mm as was horizontal, or 2.5mm in centre row G) Mold dimensions. Width (W) varies for specimens. H) Dimensions of mold insert (W varies for specimens)

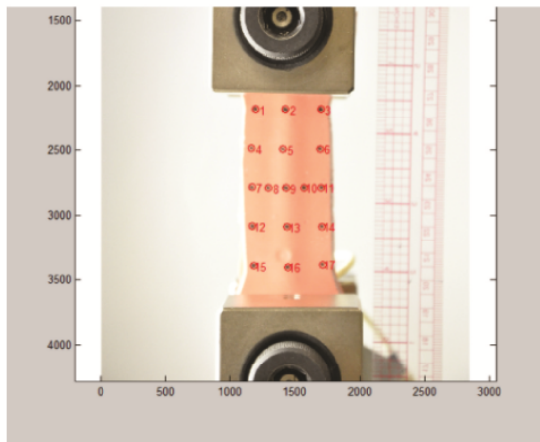
#### **4 Test Specimen Characterization**

The specimen for testing was mounted in the clamps of the tensile testing machine (Instron 5566, 2kN load cell) by manually clamping on the PDMS rigid ends of the test specimen. A remote control operated Nikon camera was positioned on a tripod at a distance of approximately 2 metres from test specimen. Automatic focus was used for the first image, and manual focus was used for subsequent images so that light settings remained constant throughout the experiment. Using a pressure regulator (Campbell Hausfeld) and a sensor (Balluff BSP000W) in line with the air supply tube, the pressure was varied in increments of 10psi and a photo was taken at each step (Figure S4A). A Matlab script was used to locate the center of each dot and output co-ordinates of the dot for each pressure increment (Figure S4B). The dots used for horizontal and vertical strain measurements are highlighted in Fig S4C.

A Representative images of Ecoflex 00-30 sample at 0psi, 20psi, 40psi



B Matlab Interface



C Vertical Strain      Horizontal Strain

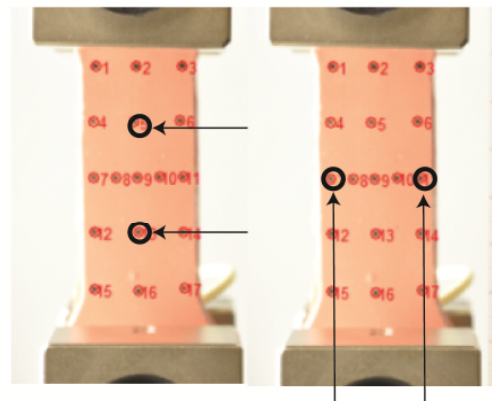
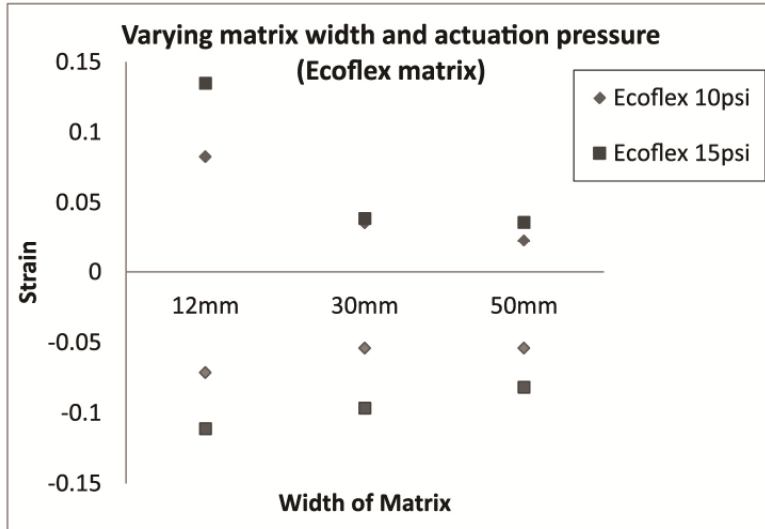


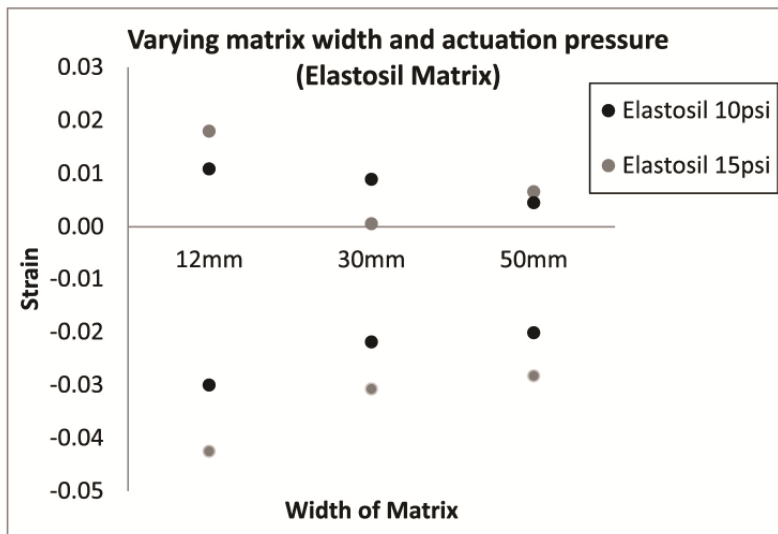
**Figure S4:** A) Representative pictures of specimens (Ecoflex 00-30, three actuators at 5mm actuator-to-actuator spacing) at 0psi, 20psi and 40psi. Supplied pressure, measured force and photos were recorded for each pressure increment B) Matlab interface used to identify and number markers and output the x,y co-ordinates of their centres to enable strain calculations. C) Markers selected for vertical and horizontal strain calculations.

## 5 Additional Results of Test Specimen Characterization

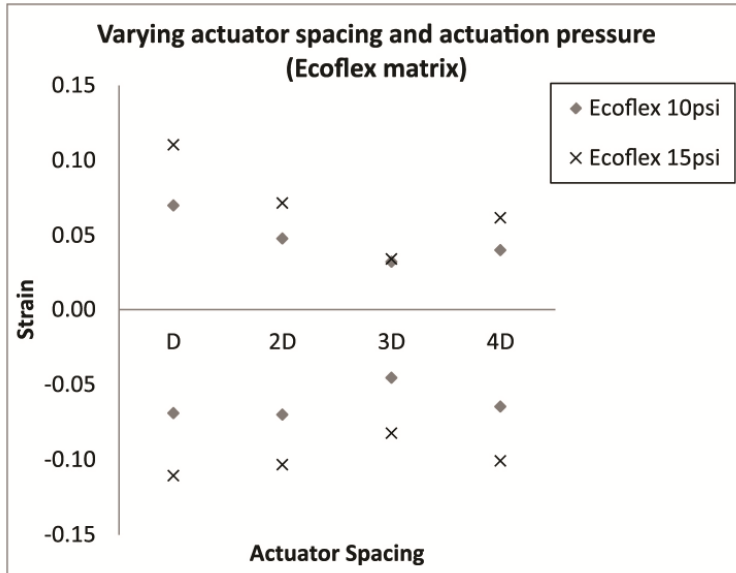
### A Single actuator specimen



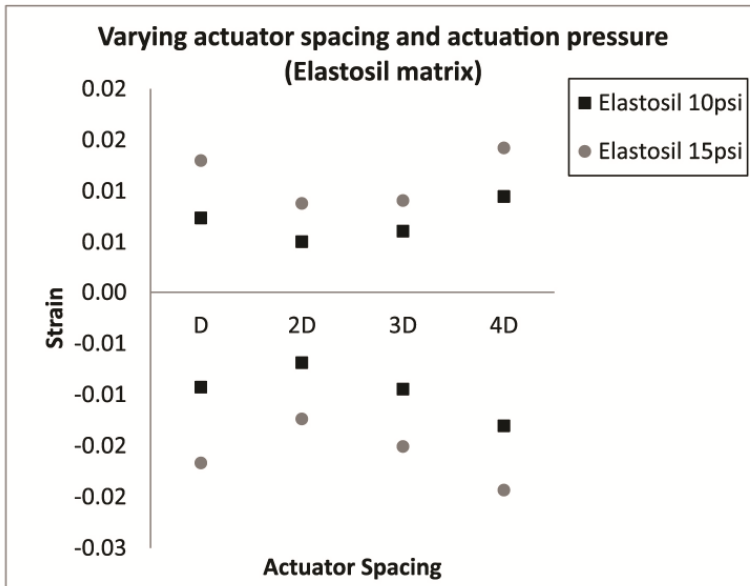
### B Single actuator specimen



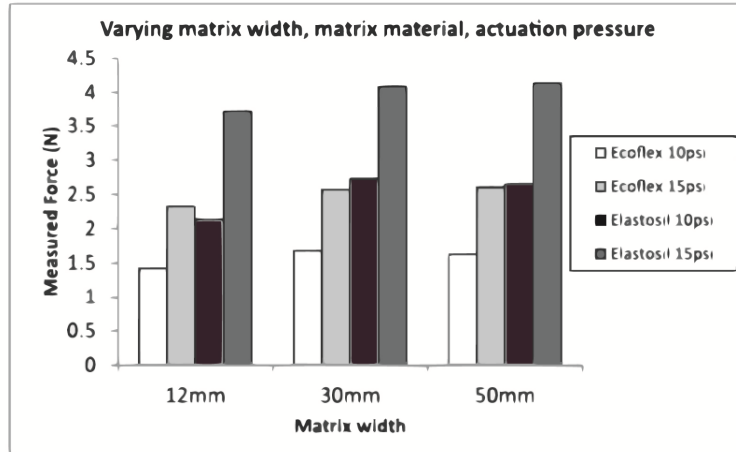
C Multiple actuator specimen



D Multiple actuator specimen



E Single actuator specimen



F Multiple actuator specimen

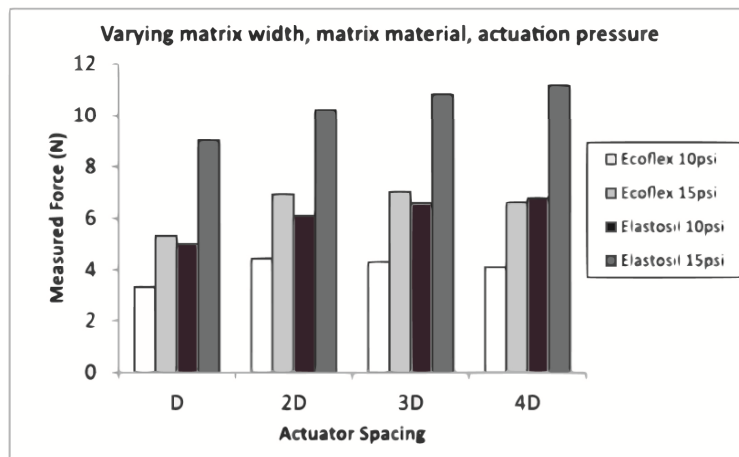


**Figure S5:** A) Strain plots for single actuator specimens with various matrix widths and pressures with Ecoflex 00-30 matrix and B) Elastosil M4601 matrix. C) Strain plots for multiple actuator specimens as a function of actuator spacing ( $D$ = nominal diameter of PAM = 5mm) with Ecoflex 00-30 matrix and D) Elastosil M4601 matrix. E) Force for single actuator specimens as a function of actuator matrix width, matrix material type and actuation pressure F) Force for multiple actuator specimens as a function of actuator spacing ( $D$ =resting diameter of PAM = 5mm), matrix material type and actuation pressure

As shown in Figure S5 varying matrix width, spacing and material affects the strain distribution and force. Although a matrix material of Elastosil can transmit a higher force (Fig S5E and Fig. S5E), our application requirement was for a high strain in a matrix with an elastic modulus in the range of myocardial tissue and so we selected Ecoflex as the matrix material (Fig S5A to Fig. S5D) because it allowed higher strains with a modulus similar to myocardial tissue. All plots in Fig S5 demonstrate that increasing actuation pressure for a given matrix width/actuator spacing/matrix material increases strain and force. In Figures S5C and S5D, for the multiple actuator specimens, strain increases when the markers are positioned directly coincident with a PAM (for example in the case where spacing= 4D). Overall, this figure demonstrates the tunable properties of our soft actuated material.

## **6 Numerical simulation of left ventricle**

Due to the 3D helical arrangement of the actuators, an additional step was required in order to assign material orientations for subsequent coefficient of expansion assignments. A 3D spline was created for the centreline of each actuator. Wire elements were temporarily assigned to these splines in order to create datums or local co-ordinate systems. Wire elements were partitioned into 22 cells perpendicular to the 3D spline in order to partition the PAMs so that an orientation could be later assigned to actuators for the orthotropic material properties described in the manuscript. Subsequently, the wire elements were deleted before merging PAMs with the matrix in the assembly module. A local co-ordinate system was defined in each of these cells so that the longitudinal axis followed the local orientation of the spline, and elements in the cell were assigned orientations according to this local coordinate system. This ensured that the longitudinal contraction and radial expansion followed the three-dimensional orientation of the muscle. The three-dimensional position of four circumferentially arranged

nodes on the inner and outer wall of each of the basal and apical planes for each actuation pressure were output. Apical rotation was calculated from these node co-ordinates using Equation 2, where the xy plane was the apical plane and the z-axis was the orthogonal axis intersecting the apex. (Figure 3b in manuscript shows these planes and the z axis as dashed blue line).

$$\theta_z = \tan^{-1}\left(\frac{y_2}{x_2}\right) - \tan^{-1}\left(\frac{y_1}{x_1}\right) [2]$$

Rotation of each of the four nodes was averaged for physiological motion (Fig 3f ), or reported independently for pathological motion (Fig 4e shows cumulative rotation of each individual node in apical plane). A total of 45,581 elements were used in the numerical simulation of the left ventricle.

## 7 Left Ventricle Fabrication

The left ventricle prototype was fabricated as described in Figure S6 below. Air supply tubes were protected with masking tape, and barbed connectors were used to connect them to an air supply for actuation.

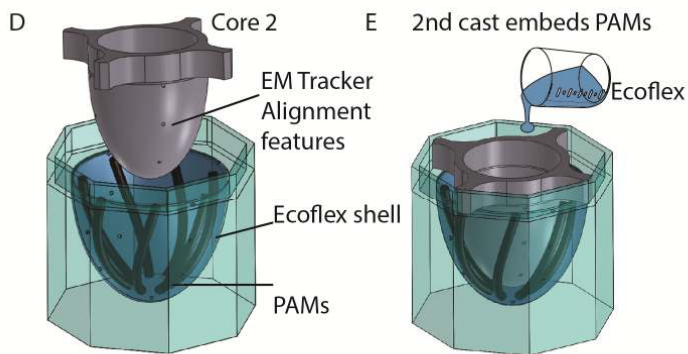
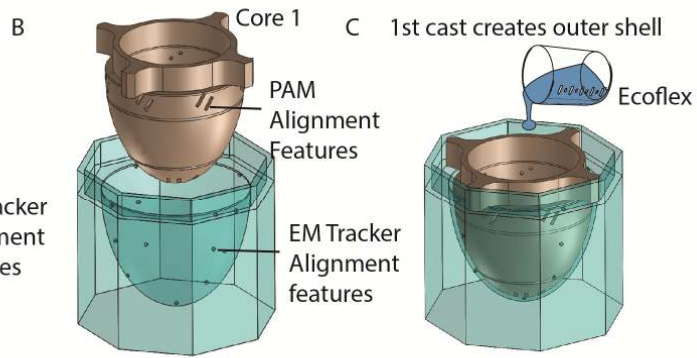
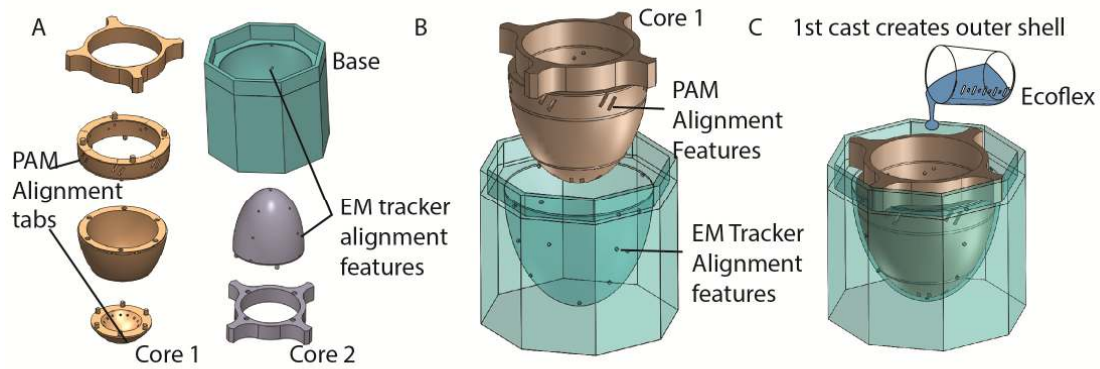
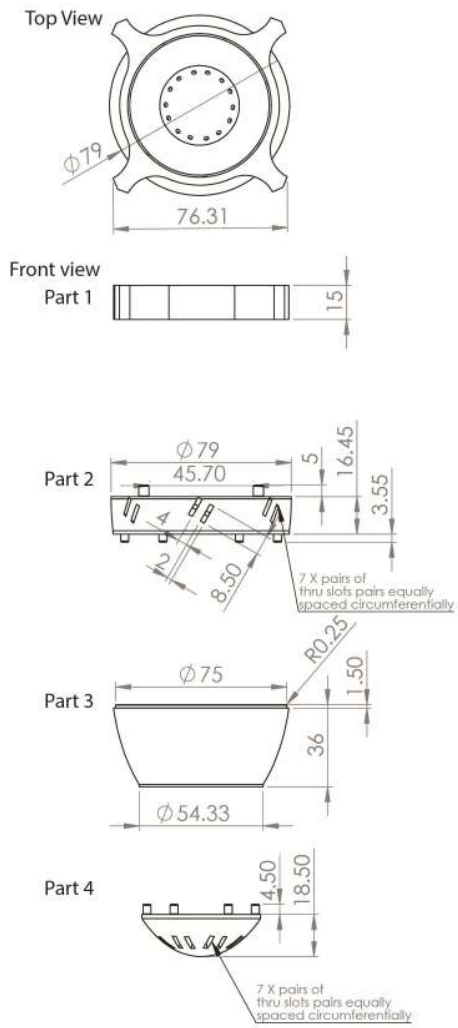


**Figure S6:** The top row for each figure shows SolidWorks models of molds with explanations on fabrication steps, while the bottom row shows photos of corresponding 3D printed molds (Object Connex vero blue) A) A multi-component reconfigurable mold B) Mold with Core 1 for casting outer shell C) 1st pour of Ecoflex 00-30 created outer shell with alignment tabs for PAMs D) With the outer Ecoflex shell remaining in mold, actuators were inserted and aligned with molded alignment features. We used a small amount of prepolymer and a heat gun to secure actuators in place and core 2 was inserted into base E) Final pour of Ecoflex 00-30 to fully embed actuators

Core 1 4 parts with reconfigurable alignment tabs



Core 2 with EM tracker alignment features

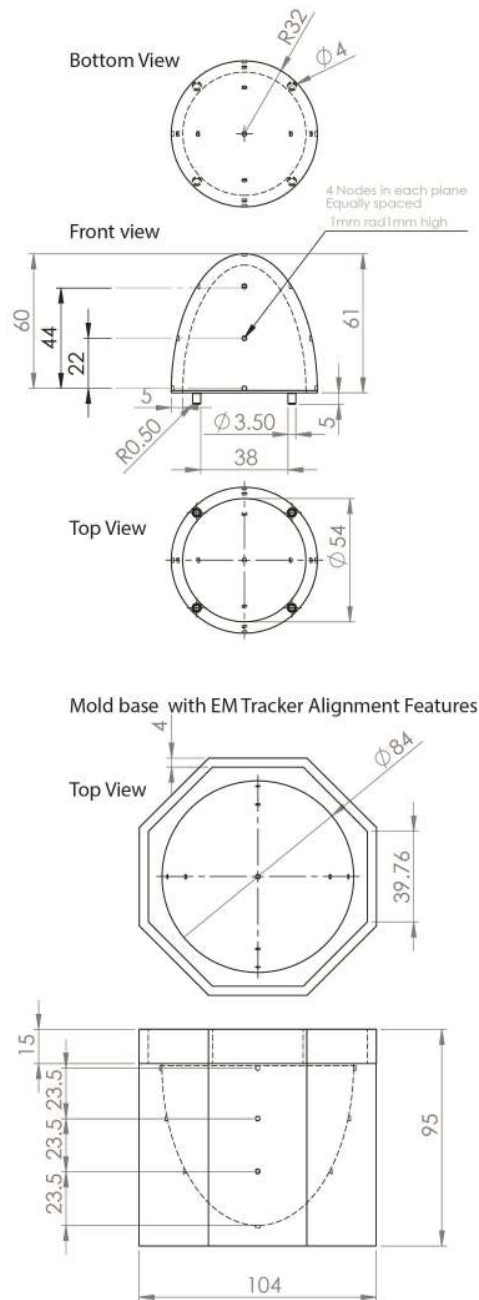
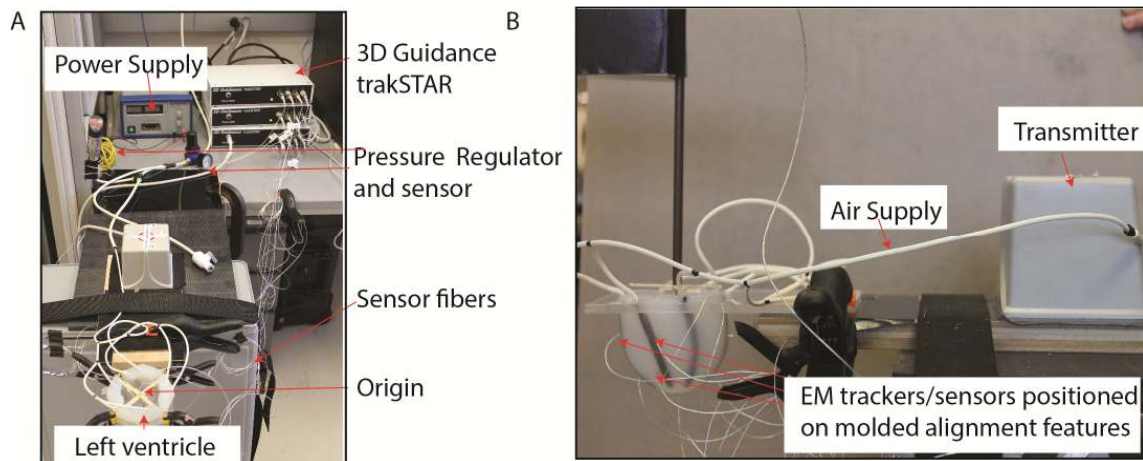


Figure S7, Dimensions of molds for making left ventricle prototype

## **8 Experimental Motion Measurement with Electromagnetic Trackers**

The experimental setup for measuring motion is described in Figure S8. A customized stand was laser cut from acrylic with a circle of diameter 82mm to support the left ventricle at the base, leaving the apex free to rotate. No metal fixtures were used to avoid interference with the electromagnetic sensors. TrakSTAR 3D Guidance system (Ascension Technologies) Model 90 6DOF freedom sensors (0.9mm) were used for displacement tracking. One sensor was fixed in the centre of the base using wooden struts. This acts as the the origin, and enabled the position of each sensor relative to this origin to be measured. The transmitter and the origin (shown in Fig. S8) were fixed. A 22 gauge needle was used to make a small hole in the centre of the molded alignment features, and sensors were advanced into the wall so the silicone self-sealed around the sensors in order for them to move with the mold. Four sensors were placed symmetrically in the outer left ventricle wall at each of the basal and apical planes (described in Fig. 3B in manuscript). Two sensors were placed in the mid plane, and an additional sensor at the apex. Information from the initial sensor readings was used to select the appropriate nodes in the finite element simulation in order to have a direct comparison. Actuation pressure was controlled with a pressure regulator (Campbell Hausfeld) and a sensor (Balluff BSP000W) in line with the air supply.



**Figure S8:** Experimental set-up for electro-magnetic tracking of left ventricle physical prototypes

Cubes software (Ascension Technology) reported the three dimensional positions of each sensors ( $x,y,z$  co-ordinates relative to the fixed origin) at each pressure increment, and a matrix of sensor co-ordinates was output to a matlab file. Sensor co-ordinates were recorded five times at each measured pressure. Apical rotation was calculated from these positional co-ordinates according to Equation 2 above. The rotation of each node was averaged for each pressure, and all four nodes in the plane were averaged for apical rotation for reported values (Fig 3f). In order to measure apical and basal rotation, the left ventricle was supported with a flexible band at the mid plane, and the readings of sensors in the apical and basal planes were used to calculate apical and basal rotation. Reported values (Fig 3f) are averages of the four nodes in each plane. For pathological motion, rotation of each node was reported independently (Fig 4f in manuscript shows cumulative rotation of each individual node in the apical plane).